

Separated Flowfield on a Slender Wing Undergoing Transient Pitching Motions

S. A. Thompson,* S. M. Batill,† and R. C. Nelson‡

University of Notre Dame, Notre Dame, Indiana 46556

An experimental investigation on the flowfield surrounding a delta wing undergoing a transient pitching motion was conducted. The leading-edge vortices were marked with smoke, and the model and vortex motions were recorded using high-speed motion picture photography. These film records were then analyzed to yield information on the vortex location and trajectory as functions of both angle of attack and time. Hysteresis effects on the vortex dynamics were apparent for both the pitch-up and pitch-down motions. The amount of lag from the static position was seen to be a function of the combined effects of nondimensional pitch rate and initial breakdown location. Reynolds number effects were inconsistent. Upon completion of the wing motion, the vortex breakdown typically would not have reached the static position, but would continue moving relative to the wing surface.

Nomenclature

c	= root chord length, in., mm
K	= nondimensional pitching frequency for transient motion, $\dot{\alpha}c/(2U)$
Re	= Reynolds number
t	= time, s
t^*	= nondimensional time, $t/\Delta t$
t^{**}	= nondimensional time, t/τ
U	= freestream velocity, f/s, m/s
x	= distance from apex of model, parallel to root chord, in., mm
α	= angle of attack, deg
$\dot{\alpha}_m$	= maximum pitch rate attained during transient motion, rad/s
α_0	= initial angle of attack, deg
Δt	= temporal duration of a specific transient pitching maneuver, s
$\Delta\alpha$	= half of the total change in angle of attack, deg
σ	= true population standard deviation
τ	= convective time, c/U , s
ω	= angular velocity of the pitch mechanism drive shaft, rad/s

Introduction and Review

THE static aerodynamic performance of slender delta wings at large angles of incidence has been the subject of numerous research studies since the earlier pioneering experiments of Peckham¹ in the mid-1950s. Since that time much has been learned about the leeward flow structure above a delta wing. Both theoretical and experimental studies have examined the formation and breakdown of the leading-edge and secondary vortices and their effect on the nonlinear aerodynamic characteristics of slender wings. Only recently have researchers started to examine the implication of unsteady wing motion on slender wing aerodynamics. A brief review of

some of the most recent studies is included in the following paragraphs.

Gad-el-Hak and Ho² performed experiments on a 45-deg sweep delta wing oscillating in pitch. They found that for an oscillation from 10–20 deg there was a difference in the vortex core position between the angle-of-attack increasing and the angle-of-attack decreasing portions of the motion. They also found that for a pitching motion of 0–30 deg the hysteresis loop in the core location was not a function of Reynolds number over the range of 25,000–340,000.

In 1988 and 1990 LeMay³ and LeMay, Batill, and Nelson^{4,5} conducted investigations into the effect of a sinusoidal pitching motion on the location of the vortex breakdown. They used a 70-deg sweep flat-plate delta wing and tested it at root chord Reynolds numbers from 90,000 to 350,000. The experiments were conducted over angle-of-attack ranges of 29–39 and 0–45 deg. By using flow visualization, LeMay et al. obtained information on both the chordwise breakdown position and the height above the wing of the breakdown, both as functions of angle of attack. They also examined the time lag between the dynamic and static positions of the vortex breakdown and found that the time lag was a function of pitch rate.

Also in 1988, Bragg and Soltani⁶ presented a study on a 70-deg sweep delta wing of geometry similar to that of the wing used in the current study. Using a constant chord Reynolds number of 1.5×10^6 , Bragg and Soltani measured the aerodynamic loads on a static wing as well as a wing undergoing sinusoidal and ramp pitching motions. Hysteretic behavior was noted in the aerodynamic loads. The magnitude of the hysteresis was found to be a function of reduced frequency and pitch rate. Lift coefficient overshoots of as much as 60% were seen. For the ramp pitching motion they observed that, after the model motion had stopped, the force and moment oscillated with small amplitude about the steady-state value before reaching equilibrium.

Another very comprehensive study on unsteady effects was conducted by Cunningham and den Boer.⁷ This study focused on a straked delta wing and combined a wide range of flow visualization, surface pressure measurements, and force and moment tests. Steady tests were conducted with angles of attack from 8 to 50 deg, and unsteady tests were performed with angles ranging from 0 to 45 deg. In addition, harmonic and spectral analyses were performed on the unsteady data. Several different flow regimes were identified, and for the unsteady data the mean angle of attack was seen to be a very influential factor. Cunningham and den Boer also demonstrated the importance of examining the results of several testing methods to clarify the complex flowfield over the

Presented as Paper 89-0194 at the AIAA 27th Aerospace Sciences Meeting, Reno, NV, Jan. 9–12, 1989; received June 29, 1989; revision received July 13, 1990; accepted for publication July 13, 1990. Copyright © 1989 by R. C. Nelson. Published by the American Institute of Aeronautics and Astronautics, Inc., with permission.

*Graduate Research Assistant, Department of Aerospace and Mechanical Engineering, Student Member AIAA.

†Associate Professor, Department of Aerospace and Mechanical Engineering, Associate Fellow AIAA.

‡Professor, Department of Aerospace and Mechanical Engineering, Associate Fellow AIAA.

straked wing. They showed that some fluctuations in surface pressure were attributable to a change in the height of the vortex core above the wing; this was due to vortex breakdown occurring downstream.

Wolffelt⁸ performed experiments on a 60-deg sweep delta wing in a water tunnel. Both harmonic pitching motions and ramp pitching motions were studied. For the ramp motions the model was pitched through a 10-deg arc at a pitch rate of 0.6 rad/s beginning at 10, 15, and 20 deg. Wolffelt noted a lag in the vortex breakdown position during the ramp motion relative to the static case. He also found that the vortex breakdown continued to move after the model had stopped, approaching the static position.

A study by Reynolds and Abtahi⁹ was performed on a 75-deg sweep delta wing in a water tunnel. The root chord Reynolds number varied from 20,000 to 65,000. They pitched the wing from 30 to 51 deg at pitch rates of 0.03–0.16 rad/s. Distinctive response characteristics were seen for the pitch-up and pitch-down cases. For the pitch-down cases, the breakdown required from 10 to 30 convective time units (defined as the chord length divided by the freestream velocity) to reach the steady-state position. Furthermore, they found that the vortex position data would correlate when nondimensionalized by the convective time.

Jarrah^{10,11} conducted a study on delta wings of aspect ratios 1, 1.5, and 2 through a Reynolds number range of 450,000–850,000. He found that, for a sinusoidal pitching motion, the hysteretic behavior of the aerodynamic coefficients was a function of the pitch rate and the aspect ratio, and the Reynolds number influence was negligible. Jarrah attributed the large overshoot of the aerodynamic loads during a pitch up (up to 50%) to a delay in the onset of vortex breakdown. Similarly, the undershoot seen during a pitch down was attributed to a delay in the transition back to a pre-breakdown vortex core.

Each of these studies has seen similar response of the vortical flow to an unsteady wing motion. Hysteretic behavior is a commonly observed characteristic. The flow has a limited ability to follow an unsteady maneuver, and a large number of convective time units are often required for the flowfield to resume its static equilibrium position. The current study was prompted by an interest in understanding how a transient motion affects the vortex breakdown location. This was accomplished using flow visualization.¹² The primary objective was to study vortex breakdown position during a transient motion.

Experimental Apparatus

Wind-Tunnel Facility and Experimental Model

This experiment was conducted using a subsonic wind tunnel located at the University of Notre Dame Aerospace Engineering Laboratory. Complete details on this facility are available in Ref. 3. The model was a flat-plate, 70-deg sweep

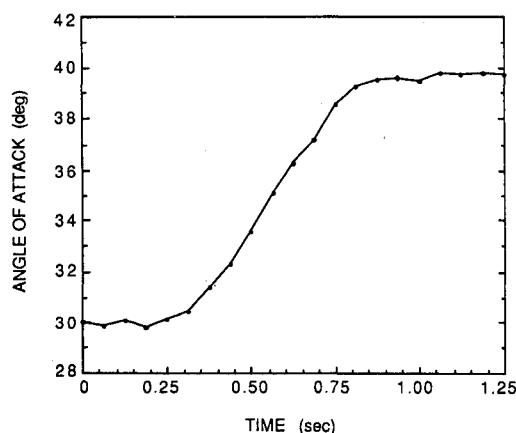


Fig. 1 Typical angle-of-attack time history.

delta wing. It had a root chord of 16.375 in. (416 mm) and a thickness of 0.5 in. (12.7 mm) and a 23-deg leading-edge bevel on both the upper and lower surfaces. Two smoke injection ports were located near the apex of the model; these two ports were placed symmetrically about the midchord. Each port was located in the center of the bevel, 1 in. from the apex; this point on the model was the most advantageous location for introducing smoke into the leading-edge vortex core.

In order to move the model in either a sinusoidal or transient pitching motion, a drive system was constructed that consisted of a constant speed motor connected to the delta-wing model by a series of linkages. This mechanism provided for different mean angles of attack and ranges of motion. By use of an electric brake/clutch, the mechanism could be put into continuous motion, or pulsed through a predetermined range of motion. Further information and a schematic of the system can be found in LeMay et al.³⁻⁵

When placed in the continuous motion mode, the pitching mechanism produces a sinusoidal variation in α . To produce the transient motion, the pitching mechanism was activated for a fixed interval to produce a $1 \pm \cos$ motion. Figure 1 shows a measured angle-of-attack time history recorded for a typical pitch-up motion. A truly "impulsive" motion would require an infinite acceleration of the model. Aircraft are not capable of truly impulsive motions; a pitching maneuver would more closely resemble a transient $1 \pm \cos$ function than a step function.

Flow Visualization Method, Data Acquisition, and Reduction

To make the core of the leading-edge vortices visible, titanium tetrachloride (TiCl_4) was introduced through the smoke injection ports.¹³ TiCl_4 reacts with the water vapor in the air to form a dense white smoke. The transient maneuvers were then recorded using a high-speed 16-mm motion picture camera. Proper lighting, control of the smoke generation process, and timing of the actuation mechanism were all important factors in this experiment.

After the experiments were conducted, the films were projected frame by frame onto a digitizing table, and the instantaneous angle-of-attack and vortex breakdown position were obtained. For a given case between three and six cycles of transient motion were filmed, digitized, and ensemble averaged for further analysis. The shape of the vortex breakdown smoke pattern was seen to vary between individual frames of a film. In some cases the fluid in the vortex core could be seen to expand suddenly from the tightly rolled core to the wider breakdown region. In other cases the vortex core would gradually fan out into the breakdown region. Schematics of these two types of breakdown regions are shown in Figs. 2 and 3. Figure 2 shows a relatively well-defined breakdown position.

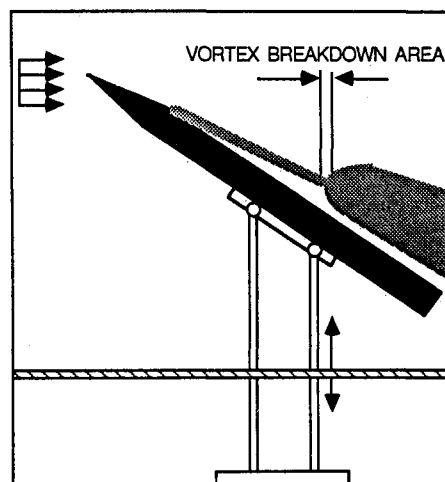


Fig. 2 Schematic of a well-defined breakdown area.

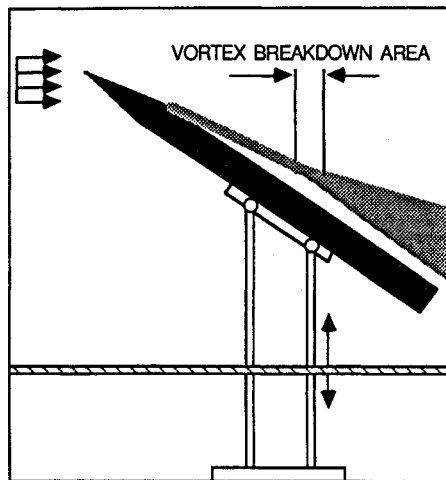


Fig. 3 Schematic of a poorly defined breakdown area.

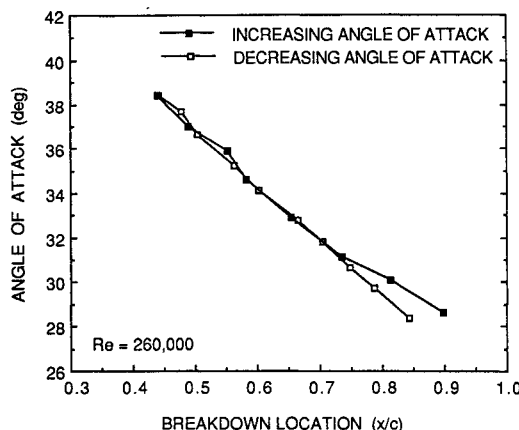


Fig. 4 Static vortex breakdown location for angle of attack increasing and decreasing.

Here the breakdown can be measured within approximately 1% of the chord length. In contrast, Fig. 3 shows a more gradual expansion. In this case the breakdown can be measured to within approximately 3% of the root chord.

Results and Discussion

Because of the nature of the data acquisition and the character of the vortex breakdown process, there are fluctuations in the position data. The variation between data records in breakdown location at a particular angle of attack is primarily a function of the breakdown motion and to a lesser extent the data reduction process. The scatter due to the data reduction process was typically much less than that due to the unsteadiness of the vortex breakdown. It was found by repeated analysis that the angle of attack was accurate to within 0.3 deg and the identification of the breakdown location was repeatable to within 0.02c. However, at a static angle of attack, breakdown was seen to vary by as much as 0.03c. For a given experiment consisting of several cycles, the standard deviation σ of the data was computed during the averaging process. The standard deviation of the angle-of-attack data ranged from $\sigma=0.13$ to 0.30 deg. For the chordwise breakdown position, σ ranged from 0.012 to 0.020c.

Static Data

The transient results obtained here are compared to both the static and sinusoidal results from LeMay et al.⁴ They used a model of identical dimensions and over a similar range of

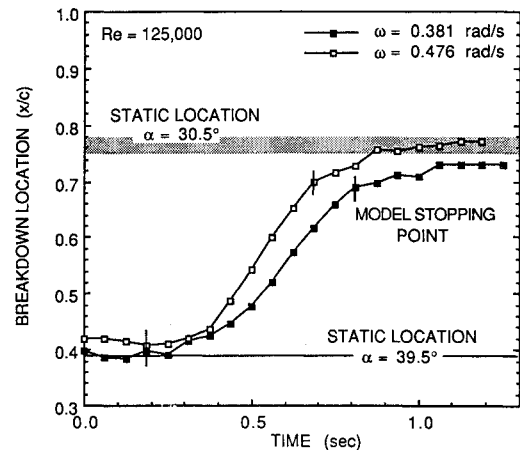


Fig. 5 Chordwise breakdown location for $Re = 125,000$ and $\omega = 0.381$ and 0.476 rad/s.

angle of attack and Reynolds number. Figure 4 shows the static data from LeMay et al.⁴ for a delta wing being pitched so that the flowfield is allowed to reach equilibrium between angles of attack from 28.5 to 38.5 deg. Figure 4 shows chordwise breakdown position plotted vs angle of attack for both increasing and decreasing angle of attack. A static hysteresis exists in the breakdown location for angles of attack from 28.5 to 31 deg.

Transient Model Motion Effect on Breakdown Location

Experiments were conducted over the angle-of-attack range of 30.5–39.5 deg. These tests encompassed root chord Reynolds numbers from 83,000 to 373,000 (corresponding to airspeeds of 10–45 ft/s or 3.05–13.72 m/s) and eight maximum pitch rates ranging from 0.317 to 0.635 rad/s. These pitch rates correspond to nondimensional pitch rates, $K = 0.078$ –0.312 [where K is defined as $\dot{\alpha}_m c / (2U)$].

Figure 5 shows the vortex breakdown position as a function of time for a pitch-down motion with constant Reynolds number and a varying maximum pitch rate. This plot represents the ensemble average of four cycles of transient motion for each case. The Reynolds number is 125,000, and maximum pitch rates of 0.381 and 0.476 rad/s are shown. The static location of the vortex breakdown at 39.5 and 30.5 deg is also shown in the figure. The static data for 39.5 deg has been extrapolated from Fig. 4.

In Fig. 5 the vortex breakdown position begins near the static location for both maximum pitch rates. Then, as the model pitches down, the breakdown moves farther down the wing, toward the trailing edge, eventually reaching its static, steady-state chordwise location. The points at which the model motion begins and ends are indicated by a data point with a vertical line through it. As would be expected, the faster pitch rate, 0.476 rad/s, results in a faster motion of the breakdown. In the 0.381-rad/s case, the last data point presented appears to have occurred before breakdown has reached the static position. The final angle of attack was the same for both cases but occurs in the range in which the static data indicates a hysteretic behavior in breakdown position. The 0.381-rad/s case seems to have reached a constant position short of the "average" static position, but, considering the possible variation associated with the static hysteresis (indicated by the shaded zone in Fig. 5) and the uncertainty in location of the breakdown position, the final breakdown locations for both cases are within the limits imposed by this experiment. To maintain clarity, the region of static hysteresis indicated in Fig. 5 has not been shown in the following figures. In place of this shaded zone is a line showing the chord location of vortex breakdown, obtained from Fig. 4. The angle-of-attack increasing or angle-of-attack decreasing portion is used appropriately.

Figure 6 presents these two data sets in nondimensional form. Both the maximum pitch rate and time have been nondimensionalized. The pitch rate has been nondimensionalized by the freestream velocity and half of the root chord. This is the same method used by Jarrah,^{10,11} Reynolds and Abtahi,⁹ and Magness et al.¹⁴ Time has been nondimensionalized by the duration of each transient maneuver. This manner of nondimensionalization is consistent throughout the remaining figures. The curves composing Fig. 5 form a single curve during the pitching motion when nondimensionalized, as indicated earlier. The nondimensional pitch rates are $K = 0.208$ and 0.260 , and the nondimensional time of the transient motion ranges from $t^* = 0$ to 1 .

Figure 7 presents similar data for a Reynolds number of $166,000$ and pitch rates of $K = 0.156, 0.208$, and 0.260 , obtained from averaging five transient pitching cycles. As with Fig. 6, the nondimensionalization of time results in the three sets of data forming a single curve during the transient motion. When the pitching motion stops, the slope of the curves (hence breakdown speed) decreases. At this point the breakdown is still forward of the static position, but it continues moving toward the static position.

This type of behavior was also seen by both Magness et al.¹⁴ and Reynolds and Abtahi.⁹ Using a 75 -deg delta wing, both groups found that, upon completion of a pitch-up or pitch-down motion, the breakdown would not have reached the static position, and that it would continue moving although at a smaller rate. Reynolds and Abtahi also found that the breakdown did not necessarily reach the static position, even 15 con-

vective time units after the completion of the event. Magness et al. found that, upon completion of the transient motion, the breakdown could move as far as half of the chord length before reaching the static position. This is consistent with Figs. 6 and 7, where the breakdown appears to reach a constant position short of the static position during the time observed. Because of the length of the data record, it is difficult to say from these two figures whether the breakdown has in fact reached a steady-state position or is moving toward the static location at a very small rate. The difference in initial breakdown position (most noticeable in Figs. 5 and 6) appears to be within the uncertainty range for this experiment.

Also evident in Fig. 7 is a slight difference in the response of the three curves upon completion of the motion, most notable for the $K = 0.260$ case. This difference in slopes after the motion is completed can also be seen in Fig. 6. Bragg and Soltani⁶ found that, at the end of a transient motion, the forces and moments would decay to a steady-state value and that this decay was a function of the pitch rate. In addition, they saw some oscillation of the aerodynamic coefficients during this decay. This characteristic also exists in the breakdown location where some oscillation can be seen in Fig. 7 for $t^* > 1.0$.

In Figs. 8 and 9 the nondimensional pitch rate is constant, and the Reynolds number is varied. The chordwise breakdown position is again plotted as a function of t^* . Figures 8 and 9 are for the same three cases; Fig. 8 is a pitch-up motion, and Fig. 9 is a pitch-down motion. Reynolds numbers of $207,000, 249,000$ and $332,000$ are shown, with a pitch rate of $K = 0.104$. For the cases shown in Fig. 8 there exists a difference in the breakdown location prior to the transient motion. This is in that range of angle of attack where hysteresis is evident in the

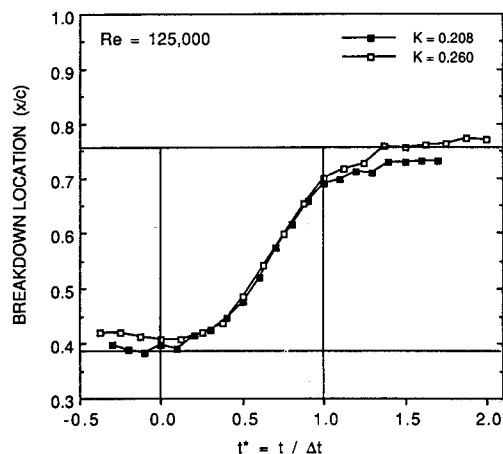


Fig. 6 Chordwise breakdown location for $Re = 125,000$ and $K = 0.208$ and 0.260 .

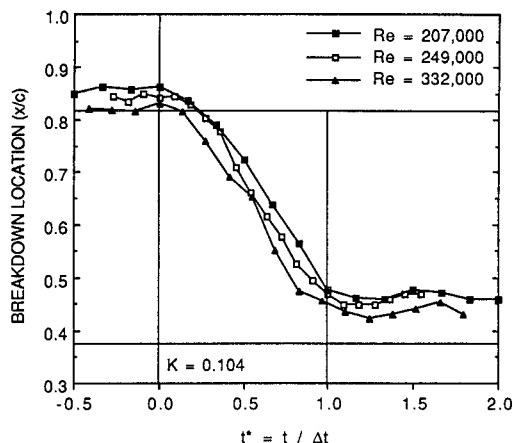


Fig. 8 Chordwise breakdown location for pitch up with $K = 0.104$ and $Re = 207,000, 249,000$, and $332,000$.

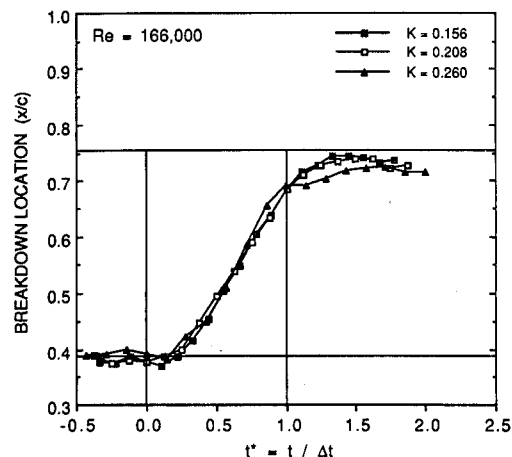


Fig. 7 Chordwise breakdown location for $Re = 166,000$ and $K = 0.156, 0.208$, and 0.260 .

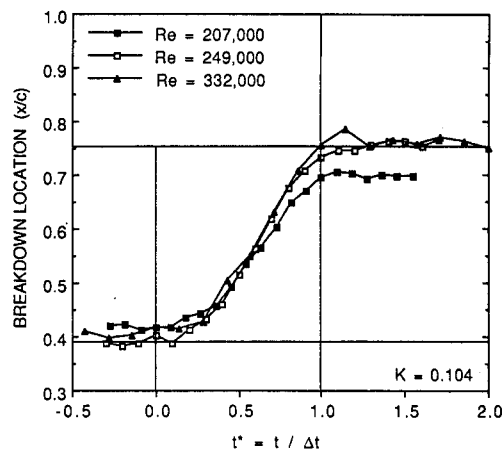


Fig. 9 Chordwise breakdown location for pitch down with $K = 0.104$ and $Re = 207,000, 249,000$, and $332,000$.

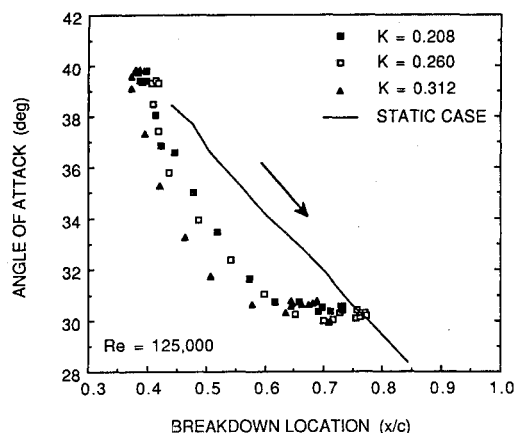


Fig. 10 Chordwise breakdown location compared to angle of attack; $Re = 125,000$; $K = 0.208, 0.260$, and 0.312 . Static case also shown.

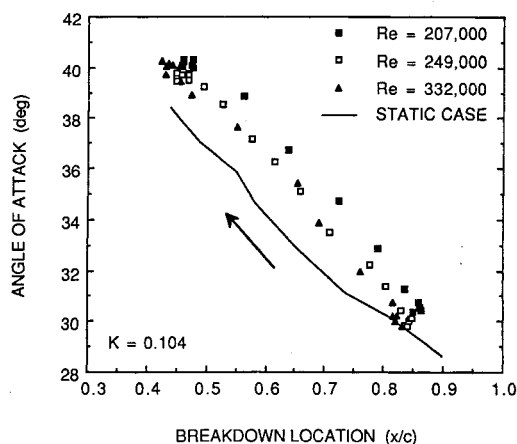


Fig. 12 Chordwise breakdown location compared to angle of attack; $K = 0.104$; $Re = 207,000, 249,000$, and $332,000$. Static case also shown.

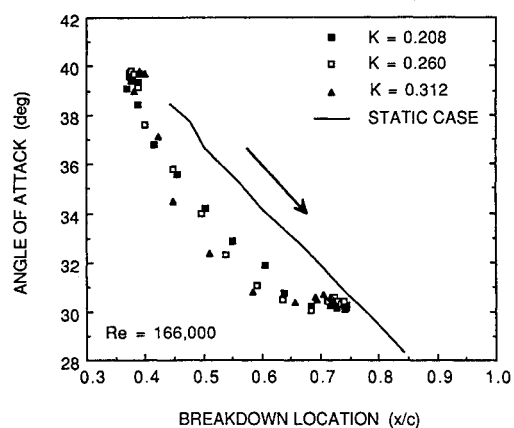


Fig. 11 Chordwise breakdown location compared to angle of attack; $Re = 166,000$; $K = 0.156, 0.208$, and 0.260 . Static case also shown.

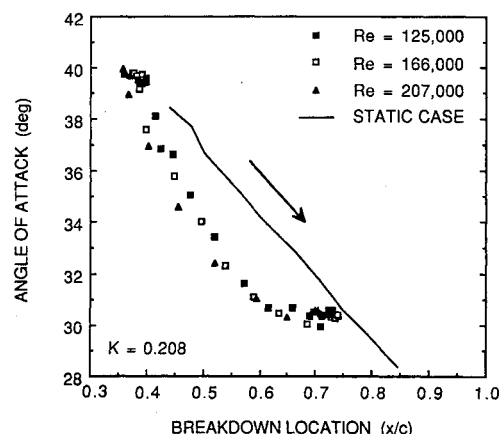


Fig. 13 Chordwise breakdown location compared to angle of attack; $K = 0.208$; $Re = 125,000, 166,000$, and $207,000$. Static case also shown.

static breakdown location. As the pitch-up maneuver begins, the breakdown moves forward on the wing. The slopes of each curve are similar. Upon completion of the motion, the rate of the breakdown position movement is significantly reduced and the expected static position was not achieved in the time interval considered. The relative position of breakdown between the three sets of data appears to be consistent throughout the event; thus, they appear to have been influenced by the difference in initial vortex breakdown position. Each of the curves in Fig. 8 is separated by roughly $0.02\text{--}0.03c$ during both the steady and unsteady parts of the plot. The difference in these three cases due to Reynolds number seems to be negligible, considering the initial difference in the breakdown location. This difference at $t^* < 0$ seems to carry over throughout the unsteady portion of the data.

Figure 9 shows the corresponding pitch-down motion. Here the initial breakdown positions are more consistent than for the pitch-up motion condition. During the maneuver the responses for the three different Reynolds numbers are similar. Some differences are noted near the end of the maneuver, at roughly $t^* = 0.8$. The case of $Re = 207,000$ shows a difference in the final breakdown position from the other two Reynolds number cases, which both appear to achieve the static breakdown location sooner. As in Fig. 7, it is possible that for this low- Re case, the breakdown is moving to the static position, but that it is moving so slowly that it is not apparent within the limited data record presented here.

In Figs. 10 and 11 the instantaneous angle of attack is presented as a function of the instantaneous chordwise breakdown location. The data represent the vortex breakdown position at a specific angle of attack as the model undergoes the

transient pitching motion. In Fig. 10 the Reynolds number is $125,000$, and the three pitch rates of $K = 0.208, 0.260$, and 0.312 are shown. The Reynolds number for Fig. 11 is $166,000$, and the pitch rates shown are $K = 0.156, 0.208$, and 0.260 rad/s. Included in these figures is the static breakdown position from LeMay.³ Those static data were taken from $28.5\text{--}38.5$ deg, and the current data are from $30.5\text{--}39.5$ deg. For this reason, in Figs. 10 and 11 the static curve extends beyond the transient data points at the low angles of attack but does not reach the transient data points at the high angles of attack.

In Fig. 10 the same pitch-down case is shown as those in Figs. 5 and 6. At the higher angles of attack, the data points are clustered around where the static position would be assuming a linear extrapolation of LeMay's data. The extent of the fluctuation of the breakdown location at a constant angle of attack can be seen near the beginning of the maneuver since some data prior to the initiation of the event are included. As the model pitches, the breakdown position moves back on the wing, lagging the static position. It can be seen from Fig. 10 that an increase in the pitch rate causes an increase in the lag of the breakdown position from the static position. Bragg and Soltani⁶ found the forces and moments to be a function of the pitch rate. Upon completion of the motion, the data show a roughly constant angle of attack; the slight variation is due to the uncertainty in the angle-of-attack measurement (the model is in fact at a constant attack angle). At the end of the event, the breakdown chord position is increasing as it moves toward the static position. The case of $K = 0.260$ appears to have had sufficient time to reach the static position; however, the other

two cases do not reach the average static position before the data record was stopped. The characteristics shown in Fig. 11 are similar to those in Fig. 10, although they are for a slightly higher Reynolds number (166,000). As the model is pitched down, the breakdown lags the static position, with the amount of this lag increasing for increasing nondimensional pitch rate. Again, the end of the maneuver leaves the breakdown forward of the static position, but gradually moving toward it. For these cases shown in Fig. 11, the final data point puts the breakdown within 5% of the static position.

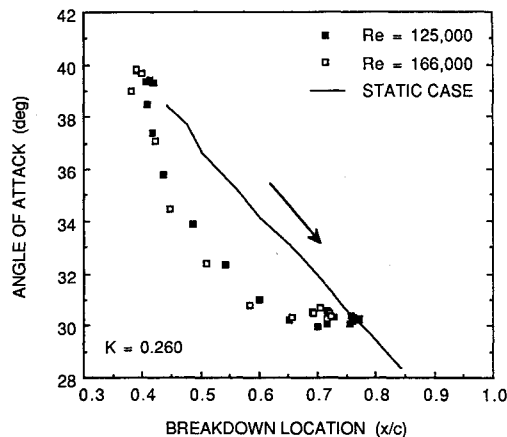


Fig. 14 Chordwise breakdown location compared to angle of attack; $K = 0.260$; $Re = 125,000$ and $166,000$. Static case also shown.

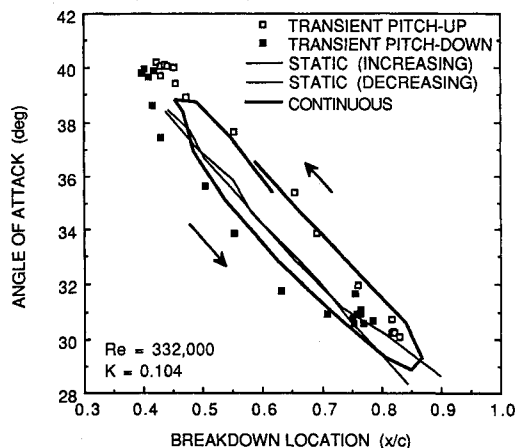


Fig. 15 Comparison of transient motion data to sinusoidal motion data and static data; $Re = 332,000$.

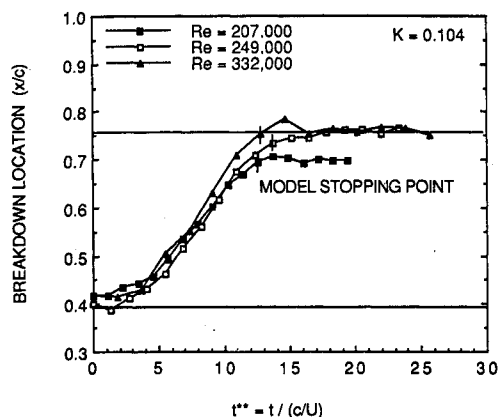


Fig. 16 Chordwise breakdown location as a function of nondimensional time $t^{**} = t/(c/U)$; $K = 0.104$; $Re = 207,000$, $249,000$, and $332,000$.

Figures 12–14 also contain data for angle of attack as a function of breakdown location, but for a constant nondimensional pitch rate and varying Reynolds number. Figure 12 is for a pitch-up condition whereas Figs. 13 and 14 are for a pitch-down condition. Nondimensional pitch rates of $K = 0.104$, 0.208 , and 0.260 and the static case are shown.

At the beginning of the event, in Fig. 12, the breakdown position is consistent with the static data. As the model pitches up, the breakdown position lags the static curve by as much as 15% of the chord for the low- Re case. As the model comes to a halt, the rate at which the breakdown moves decreases, and the breakdown moves slowly forward toward the static position until the end of the data record.

Figure 13 shows a pitch-down motion for $K = 0.208$ and three Reynolds numbers. Characteristics similar to those of Fig. 12 are seen. The amount of lag during the maneuver is similar in magnitude to that of Fig. 12, about 18% of the chord at most. Figure 14 shows similar characteristics. This figure is for a higher nondimensional pitch rate, $K = 0.260$, but the amount of lag of the breakdown from the static position still has a maximum of about 18%. The lower Re case, $Re = 125,000$, reaches the static position by the end of the data record. The higher Re case seems to reach a constant chord position about $0.04c$ forward of the average static position, but this is in the region of the static position hysteresis.

Typically, delta-wing vortex flows are considered to be independent of Reynolds number, although past researchers have seen Reynolds number effects.^{3,9} Throughout Figs. 12–14, there was no apparent effect due to the Reynolds number, although the Reynolds number range was small. This also applies to Figs. 8 and 9. Figure 8 shows a difference, but this is more likely due to a difference in the initial breakdown location.

Figure 15 is a comparison of the breakdown position for transient motion and for sinusoidal motion (the sinusoidal data obtained from LeMay³). In addition, the static data are shown for both increasing and decreasing angles of attack. It is important to note that the sinusoidal data (as well as the static data) span a somewhat different range of angles of attack than the transient data. The curves in Fig. 15 are for a Reynolds number of 332,000 (40 ft/s, 12.2 m/s). The maximum pitch rate for both the transient and the sinusoidal motion is the same; that is, if during the transient motion the model had been allowed to continue pitching, the angular frequency would have corresponded to the sinusoidal case shown in Fig. 15. From Fig. 15 the pitch-up case can be seen to follow the upstroke of the continuous motion, whereas the transient pitch-down location slightly lags the downstroke of the continuous motion. Reynolds and Abtahi⁹ also noted a difference between the responses for transient upstroke and transient downstroke maneuvers. Bragg and Soltani⁶ also found a difference in the force and moment between the upstroke and the downstroke motions.

Another method of nondimensionalization was performed by using the convective time τ . The three data sets from Fig. 9 are presented in this manner in Fig. 16, which contains three cases with different Reynolds numbers and the same nondimensional pitch rate of $K = 0.104$. Nondimensional time is here defined as $t^{**} = t/\tau$. The data records have been truncated so that $t^{**} = 0.0$ corresponds to the beginning of the transient event. However, the end of the motion takes place from $t^{**} = 12.6$ – 13.7 convective time units, and for each case it is noted with a flag on the last data point during the maneuver. From this point it takes approximately five more convective time units for the two higher Re cases, which correspond to higher freestream velocity, to reach the static position. After eight convective time units, the low-speed case ($Re = 207,000$) has not yet reached the static position and appears to have reached a constant position roughly 6% of the chord length from the static line. This is again in the region of considerable static position hysteresis. However, Reynolds and Abtahi⁹ found that convective times of up to 30 were neces-

sary for breakdown to reach the static position. As such, the difference of 0.06c after only eight convective time units seems reasonable.

Conclusions

The characteristics of the vortex breakdown over a 70-deg sweep delta wing during a transient pitching maneuver were examined for several pitch rates and Reynolds numbers. Significant hysteresis effects are apparent. The response of the breakdown to the transient motion was seen to be dependent on a combination of factors, including nondimensional pitch rate, initial breakdown location, and direction of motion. There exists some difficulty in separating the influence of each of these factors.

The instantaneous response of the breakdown location was seen to lag the corresponding static location for a specific angle of attack. The pitch rate was the key factor in determining the ability of the breakdown to respond to the unsteady motion. As the nondimensional pitch rate increased, the amount of lag between the transient and static positions increased. No consistent Reynolds number effect was seen, although the range of Reynolds numbers tested was small and previous researchers have seen such effects in unsteady data.

It was also seen that the transient vortex breakdown location continues to move toward the static breakdown location upon completion of the transient maneuver. Typically the breakdown would cover at least 80% of the distance between static locations by the time the pitching motion was completed. For some cases the breakdown would continue moving at a much smaller rate, and in some cases it appeared that the breakdown had reached a constant chord position. However, other research has shown that large convective time units can be necessary for the breakdown to reach its final equilibrium position; it is possible that the data records of the current study were not long enough to detect the continued motion of the breakdown. Furthermore, upon completion of the maneuver, the rate at which the breakdown moves toward the static position appears to be a function of the pitch rate. This has also been shown to be true for the aerodynamic forces and moments.

The pitch-down response and the pitch-up response were not necessarily the same, nor were they the same when compared to a continuous, sinusoidal pitching motion. Differences in the vortical flow during the upstroke and downstroke motions result in a difference in the breakdown location, as well as in the aerodynamic coefficients, as shown by other investigators.

Any static hysteresis that exists could also play a part in shifting the location of the breakdown during a transient maneuver. If the model begins a transient motion with the breakdown at a position different than the static position, the response of the breakdown during the maneuver will be different. This can occur if sufficient time is not allowed for the breakdown to reach the static position before a new tran-

sient motion is initiated. This detrimental effect could be compounded as several transient pitching motions are made, each time with the breakdown location starting from a different static position.

Acknowledgments

This research was sponsored by the University of Notre Dame Department of Mechanical and Aerospace Engineering and NASA Langley Research Center, Hampton, Virginia, under Grant NAG-1-727. Jay Brandon was the NASA Technical Monitor for this research grant.

References

- ¹Peckham, D. H., "Low Speed Wind Tunnel Tests on a Series of Uncambered Slender Pointed Wings with Sharp Edges," Aeronautical Research Council, London, Reports and Memoranda, No. 3186, April 1958.
- ²Gad-el-Hak, M., and Ho., C. M., "The Pitching Delta Wing," *AIAA Journal*, Vol. 23, No. 11, 1985, pp. 1660-1665.
- ³LeMay, S. P., "Leading Edge Vortex Dynamics on a Pitching Delta Wing," M.S. Thesis, University of Notre Dame, Notre Dame, IN, April 1988.
- ⁴LeMay, S. P., Batill, S. M., and Nelson, R. C., "Vortex Dynamics on a Pitching Delta Wing," *Journal of Aircraft*, Vol. 27, No. 2, 1990, pp. 131-138.
- ⁵LeMay, S. P., Batill, S. M., and Nelson, R. C., "Leading Edge Vortex Dynamics on a Pitching Delta Wing," AIAA Paper 88-2559, June 1988.
- ⁶Bragg, M. B., and Soltani, M. R., "An Experimental Study of the Effect of Asymmetrical Vortex Bursting on a Pitching Delta Wing," AIAA Paper 88-4334, Aug. 1988.
- ⁷Cunningham, A. M., Jr., and den Boer, R. G., "Low-Speed Unsteady Aerodynamics of a Pitching Straked Wing at High Incidence—Part II: Harmonic Analysis," *Journal of Aircraft*, Vol. 27, No. 1, 1990, pp. 31-41.
- ⁸Wolffelt, K. W., "Investigation of the Movement of Vortex Burst Position with Dynamically Changing Angle of Attack for a Schematic Delta Wing in a Water Tunnel with Correlation to Similar Studies in Wind Tunnel," AGARD Paper CPP-413, Oct. 1986.
- ⁹Reynolds, G. A., and Abtahi, A. A., "Instabilities in Leading-Edge Vortex Development," AIAA Paper 87-2424, Aug. 1987.
- ¹⁰Jarrah, M. A. M., "Unsteady Aerodynamics of Delta Wings Performing Maneuvers to High Angle of Attack," Ph.D. Dissertation, Stanford University, Stanford, CA, Dec. 1988.
- ¹¹Jarrah, M. A. M., "Low-Speed Wind-Tunnel Investigation of Flow About Delta Wings, Oscillating in Pitch to Very High Angle of Attack," AIAA Paper 89-0295, Jan. 1989.
- ¹²Thompson, S. A., Batill, S. M., and Nelson, R. C., "The Separated Flow Field on a Slender Wing Undergoing Transient Pitching Motions," AIAA Paper 89-0194, Jan. 1989.
- ¹³Visser, K. D., Ng, T., and Nelson, R. C., "Method of Cold Smoke Generation for Vortex Core Tagging," *Journal of Aircraft*, Vol. 25, No. 11, 1988, pp. 1069-1071.
- ¹⁴Magness, C., Robinson, O., and Rockwell, D., "Control of Leading-Edge Vortices on a Delta Wing," AIAA Paper 89-0999, March 1989.